



## Lau visibility sensor

Cristina M. Gómez-Sarabia<sup>a</sup>, Luis M. Ledesma-Carrillo<sup>b</sup>, Jorge Ojeda-Castañeda<sup>c,\*</sup>

<sup>a</sup> Digital Arts, DICIS, University of Guanajuato, Salamanca, 36885, Mexico

<sup>b</sup> Multidisciplinary Studies, DICIS, University of Guanajuato, Yuriria, 36885, Mexico

<sup>c</sup> Electrical Engineering, DICIS, University of Guanajuato, Salamanca, 36885, Mexico

### ARTICLE INFO

#### Keywords:

Lau effect  
Noncoherent Talbot effect  
Optical sensors  
Random processes

### ABSTRACT

For describing the visibility of the Lau fringes, we define complex visibility function. This definition is useful for assigning tolerances to the geometrical bends of an incoherent slit source. We relate this definition to the characteristic function of a random process, for assigning tolerances to the locations of a random set of mutually incoherent point sources. We apply our results for analyzing the temporal mismatches between the period of the harmonic motion, of a point source, and the detector average time. Several numerical simulations are included.

### 1. Introduction

For analyzing several interferometric devices, Michelson introduced the concept of visibility [1]. For defining and measuring the degree of coherence, of a planar source, Zernike proposed to apply the concept of visibility, when analyzing the interference pattern of Young's double slit experiment [2]. Hopkins corrected and extended the previous treatment, for discussing stellar interferometry, the illumination in optical microscopy and for describing a general theory of image formation [3].

As depicted in Fig. 1(a), Zernike's proposal can be applied for heuristically describing the use of a set of mutually incoherent point sources, for obtaining Young interference patterns with visibility equal to unity [4]. And as depicted in Fig. 1(b), this heuristic treatment can be easily extended to the use of a binary grating covering a spatially noncoherent source. The next step, for heuristically describing the Lau effect [5], is to substitute the double slit by a binary grating.

There are, of course, several other treatments of Lau effect [6–10]. These descriptions employ sound mathematical formulations, within the current knowledge of the optical sciences. However, from our viewpoint, these treatments omit to describe the visibility variations of the Lau patterns.

As an exception, to the above statement, we note the description of the Lau effect as a noncoherent version of the Talbot effect [11]. As well as the other reports indicating that the Lau patterns exhibits a high sensitivity to the angular misalignment of the composing gratings [12–15].

Here, our aim is to understand and to apply the visibility variations of the Lau fringes for setting a Lau sensor. To this end, we analyze the visibility variations that are caused for three different illumination architectures.

First, we define a complex visibility function that relates the modulation of the Lau fringes with the bends on an incoherent slit source. Second, we link the random locations of a cluster of mutually incoherent point sources with the visibility of the Lau fringes. Third, when gathering long exposure pictures, we describe the visibility variations produced by a point source, which follows a harmonic motion in the source plane.

In Section 2, we exploit the formation of a self-image for obtaining the deterministic *optical transfer function* (OTF) of the Lau effect. Next, we discuss the visibility variations produced by a geometrically distorted noncoherent, slit source.

In Section 3, we obtain the ensemble average OTF, of the Lau effect, for analyzing the visibility variations generated by the random locations of a cluster of mutually incoherent point sources. We show that the visibility function is proportional to the characteristic function, of the random process, which is the Fourier transform of the probability density function [16]. We discuss the visibility functions that are associated to three different probability density functions.

In Section 4, we obtain the time average OTF of the Lau effect, for discussing the visibility variations of the Lau fringes, if a point source moves harmonically inside the source plane. We propose to use this type of visibility variations for setting a null test that senses any mismatches between the averaging time  $\tau$  and the time period  $T$ ; in a somehow similar technique to stroboscopic illumination [17]. In Section 5, we summarize our contribution.

### 2. Deterministic OTF and slit distortions

In Fig. 2 we depict a single lens optical setup for discussing the Lau effect as noncoherent imaging process between the source and the

\* Corresponding author.

E-mail address: [jojedacas@ugto.mx](mailto:jojedacas@ugto.mx) (J. Ojeda-Castañeda).

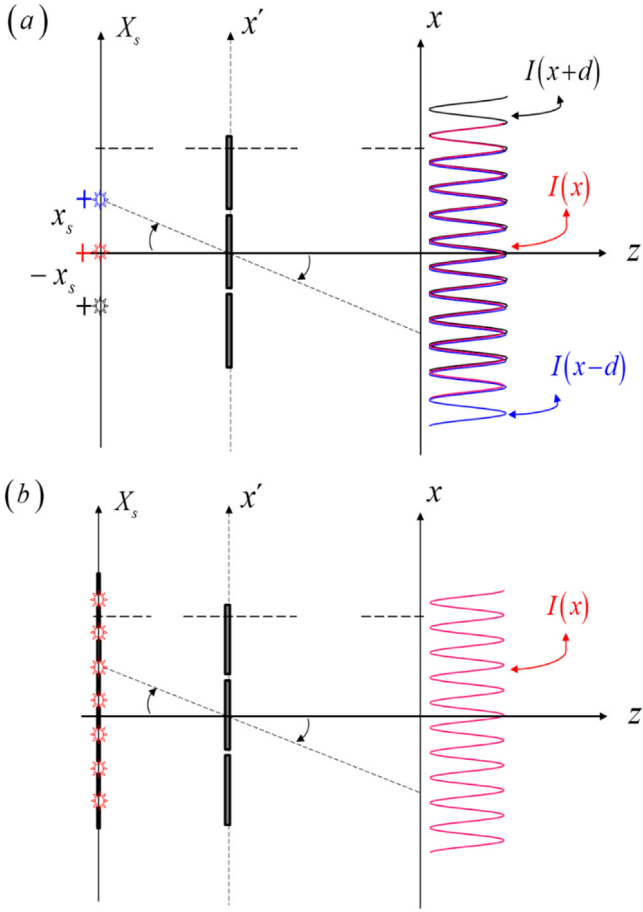


Fig. 1. In-register superposition of Young fringes. The point sources are spatially incoherent, even when they have the same wave length. In (a) we employ three different colors (despite that the wave length is the same) for depicting the in-register superposition of three shifted irradiance distributions. In (b) we illustrate the use of several spatially incoherent point sources for achieving an in-register superposition of Young fringes. (For interpretation of the references to color in this figure legend, the reader is referred to the web version of this article.)

first Talbot plane. At its front focal plane, we place a point source. Hence, a plane wavefront illuminates a sinusoidal grating that is located in close contact to a positive lens. We assume that the period of the sinusoidal grating is  $d$ . Then just behind the lens, the complex amplitude distribution is

$$g(x', y') = \cos\left(2\pi \frac{x'}{d}\right). \quad (1)$$

Under the paraxial regime, at the Talbot distance  $z = Z_T = (2 d^2/\lambda)$ , the complex amplitude distribution of the Fresnel diffraction pattern is

$$u\left(x, y, \frac{2d^2}{\lambda}\right) = \cos\left(2\pi \frac{x}{d}\right). \quad (2)$$

The irradiance distribution, at the first Talbot image, can be thought of as **irradiance point spread function** (PSF) of the Lau effect. That is,

$$h(x, y) = \left|u\left(x, y, \frac{2d^2}{\lambda}\right)\right|^2 = \frac{1}{2} \left[1 + \cos\left(4\pi \frac{x}{d}\right)\right]. \quad (3)$$

Hence, the **deterministic optical transfer function** (OTF) of the Lau effect is

$$H(\mu, \nu) = \int_{-\infty}^{\infty} \int_{-\infty}^{\infty} h(x, y) \exp[-i2\pi(\mu x + \nu y)] dx dy \quad (4)$$

$$H(\mu, \nu) = \frac{1}{2} \delta(\mu) \delta(\nu) + \frac{1}{4} \left[ \delta\left(\mu + \frac{2}{d}\right) + \delta\left(\mu - \frac{2}{d}\right) \right] \delta(\nu).$$

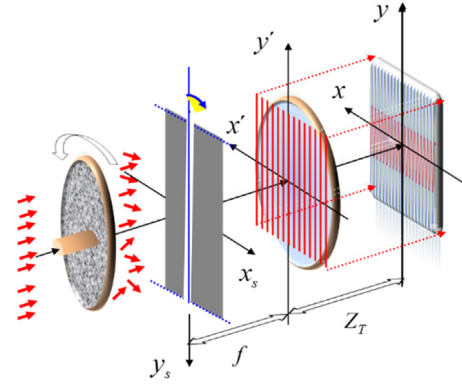


Fig. 2. Schematics of a simple optical setup for implementing the Lau effect.

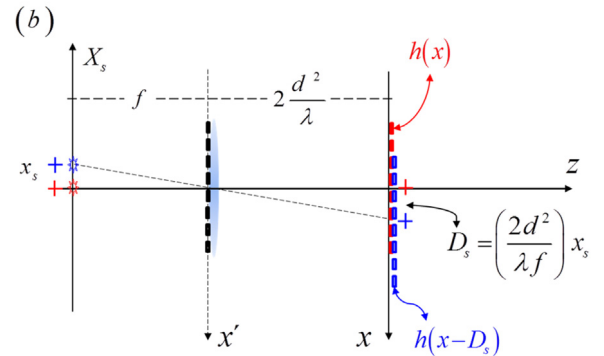
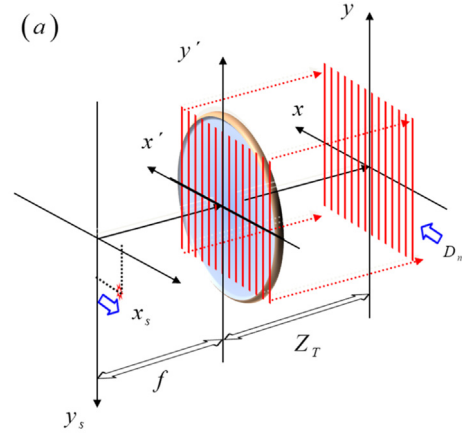


Fig. 3. Geometrical sketches for relating the lateral displacement of a point source with the lateral shift of the irradiance PSF.

Now, we consider that the input point source is displaced to a new position, say  $(x_s, y_s)$ , inside the source plane

As is depicted in Fig. 3, from simple geometric considerations, the irradiance distribution is shifted horizontally by the distance

$$D_s = \left(\frac{2d^2}{\lambda f}\right) x_s = M x_s. \quad (5)$$

In Eq. (5), the capital letter M denotes the geometrical magnification of the imaging process under discussion. The Fourier transform of the shifted PSF describes the following OTF

$$H(\mu, \nu; \beta) = \frac{1}{2} \delta(\mu) \delta(\nu) + \frac{1}{4} \delta\left(\mu + \frac{2}{d}\right) \delta(\nu) \exp(i2\pi \beta x_s) + \frac{1}{4} \delta\left(\mu - \frac{2}{d}\right) \delta(\nu) \exp(-i2\pi \beta x_s). \quad (6)$$

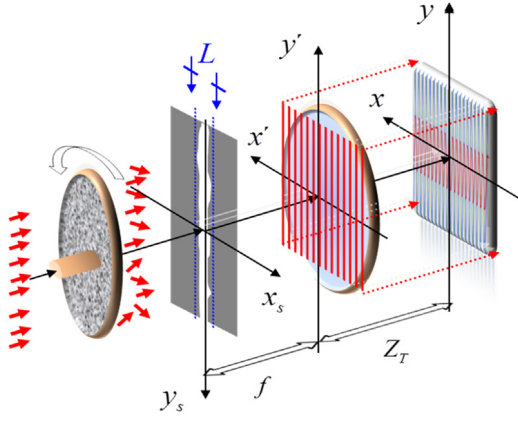


Fig. 4. Formation of the Lau fringes when using a geometrically distorted slit under noncoherent illumination.

In Eq. (6) we use the Greek letter  $\beta$  for representing the spatial frequency

$$\beta = \left( \frac{4d}{\lambda f} \right). \quad (7)$$

Next, as depicted in Fig. 4, we assume that the noncoherent source is a distorted slit. The irradiance distribution is represented by a narrow slit along the horizontal axis. The width of the horizontal window changes along the vertical axis; and the maximum width is equal to  $L$ .

Additionally, the center of the horizontal window follows the in-plane trajectory  $F(y_s)$ . Along the vertical axis, the geometrically distorted slit has width equal to  $Y$ . In mathematical terms, the normalized source irradiance distribution is

$$I_0(x_s, y_s) = \frac{1}{Y} \text{rect}\left(\frac{y_s}{Y}\right) \delta[x_s - F(y_s)]. \quad (8)$$

The new Fourier spectrum reads

$$I_0(\mu, \nu) = \frac{1}{L} \int_{-\infty}^{\infty} \text{rect}\left(\frac{y_s}{Y}\right) \exp\{-i2\pi[\mu F(y_s)]\} dy_s. \quad (9)$$

Hence, the new Fourier spectrum, of the Lau fringes is

$$\tilde{I}(\mu, \nu) = H(\mu, \nu) \tilde{I}_0(M\mu, M\nu). \quad (10)$$

In Eq. (10) the capital letter  $M$  denotes, as before, the magnification of the imaging system. If we employ the deterministic OTF in Eq. (4), then the Fourier spectrum of the Lau fringes reads

$$\begin{aligned} \tilde{I}(\mu, \nu) &= \frac{1}{2} \delta(\mu) \delta(\nu) \\ &+ \frac{1}{4} \delta\left(\mu + \frac{2}{d}\right) \delta(\nu) \int_{-\infty}^{\infty} \text{rect}\left(\frac{y_s}{Y}\right) \exp\{i2\pi[\mu M F(y_s)]\} dy_s + \\ &+ \frac{1}{4} \delta\left(\mu - \frac{2}{d}\right) \delta(\nu) \int_{-\infty}^{\infty} \text{rect}\left(\frac{y_s}{Y}\right) \exp\{-i2\pi[\mu M F(y_s)]\} dy_s. \end{aligned} \quad (11)$$

Hence, the irradiance distribution of the Lau fringes is

$$I(x, y) = \frac{1}{2} + \frac{1}{2} \text{Re} \left\{ \exp\left(i4\pi \frac{x}{d}\right) \frac{1}{Y} \int_{-\frac{Y}{2}}^{\frac{Y}{2}} \exp\{-i2\pi[\beta F(y_s)]\} dy_s \right\}. \quad (12)$$

Here, it is convenient to define the following complex visibility function

$$\gamma(\beta) = \frac{1}{Y} \int_{-\frac{Y}{2}}^{\frac{Y}{2}} \exp\{-i2\pi\beta F(y_s)\} dy_s. \quad (13)$$

The result in Eq. (13) can be readily applied to describe, as a particular case, a well-shaped, noncoherent slit source, which is tilted by an angle  $\theta$ , with respect to the vertical axis. In this particular case,

$$F(y_s) = [\tan(\theta)] y_s. \quad (14)$$

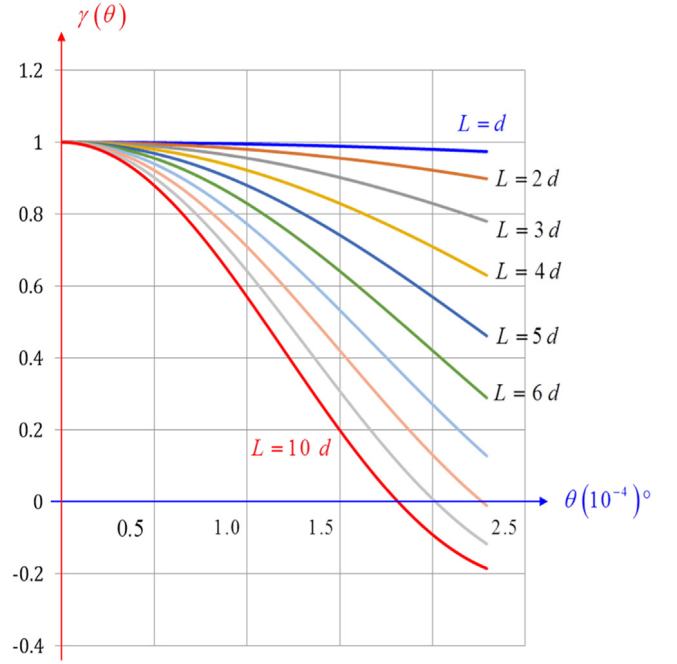


Fig. 5. Visibility function of the Lau fringes for an in-plane rotated, by an angle  $\theta$ , noncoherent slit source.

By substituting Eq. (14) in Eq. (13), we obtain that for the tilted noncoherent, slit source, the visibility reads

$$\gamma(\theta) = \text{sinc} \left[ \frac{4d}{\lambda f} Y \tan(\theta) \right]. \quad (15)$$

In Fig. 5, we plot Eq. (15) for displaying the visibility variations as a function of the tilt angle  $\theta$ . We employ curves, in different colors, for showing the parametric variation of the maximum horizontal width  $L$ , as multiple numbers of the grating period,  $d$ .

From Eq. (15), and considering the value of the first zero of the sinc function, we obtain the tolerance to angular misalignment

$$\tan(\theta) \leq \frac{\lambda f}{4Yd}. \quad (16)$$

For a grating with period equal to 1 mm,  $Y = 6$  mm, a lens with focal length  $f = 200$  mm, and for  $\lambda = 600$  nm, we have that  $\tan(\theta) \leq 0.005$ .

In Section 4, we show that for  $F(y_s) = A \sin(2\pi y/p)$ , then the visibility varies as if a point source follows a harmonic motion. However, before that we discuss *random departures* from a straight-line source. For this later purpose, it is convenient to obtain the ensemble average OTF.

### 3. Ensemble average OTF

For obtaining the *ensemble average* OTF, we consider that the lateral displacements,  $D_s$ , are produced by random locations,  $x_s$ , of a cluster of mutually incoherent point sources. By denoting the *probability density function* (PDF) of the random process as  $p_X(x_s)$ , the average OTF is

$$\begin{aligned} \langle H(\mu, \nu) \rangle &= \frac{1}{2} \delta(\mu) \delta(\nu) \int_{-\infty}^{\infty} p_X(x_s) dx_s \\ &+ \frac{1}{4} \delta\left(\mu + \frac{2}{d}\right) \delta(\nu) \int_{-\infty}^{\infty} p_X(x_s) \exp(-i2\pi\beta x_s) dx_s + \\ &+ \frac{1}{4} \delta\left(\mu - \frac{2}{d}\right) \delta(\nu) \int_{-\infty}^{\infty} p_X(x_s) \exp(i2\pi\beta x_s) dx_s. \end{aligned} \quad (17)$$

We can rewrite the result in Eq. (17) as

$$\langle H(\mu, \nu) \rangle = \frac{1}{2} \delta(\mu) \delta(\nu) + \frac{1}{4} \delta\left(\mu + \frac{2}{d}\right) \delta(\nu) P_X(\beta)$$

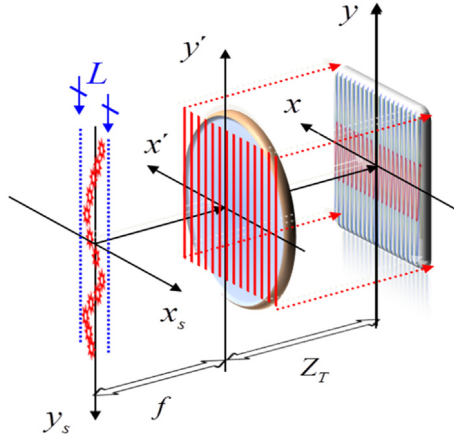


Fig. 6. Visibility reduction due to the lateral displacements of a set of mutually incoherent point sources.

$$+ \frac{1}{4} \delta \left( \mu - \frac{2}{d} \right) \delta(\nu) P_X * (\beta). \quad (18)$$

In Eq. (18), we denote as  $P_X(\beta)$  the characteristic function, which is the Fourier transform of the probability density function.

By employing the notation  $\text{Re}\{z\}$  that represents taking the real part of a complex number  $z$ , we have that the average PSF is

$$\langle h(x, y) \rangle = \frac{1}{2} + \frac{1}{2} \text{Re} \left\{ P_X(\beta) \exp \left( i 4\pi \frac{x}{d} \right) \right\}. \quad (19)$$

It is convenient now to define the complex visibility function of the Lau fringes as

$$\gamma \left( \frac{2d}{\lambda f} \right) = \left| P_X \left( \frac{2d}{\lambda f} \right) \right| \exp \left[ i \theta \left( \frac{2d}{\lambda f} \right) \right]. \quad (20)$$

Using the notation in Eq. (19), we have that the average PSF is

$$\langle h(x, y) \rangle = \frac{1}{2} + \frac{1}{2} |P_X(\beta)| \cos \left[ 4\pi \left( \frac{x_0}{d} \right) + \theta(\beta) \right] \quad (21)$$

The above results are next applied for describing the visibility variations of some random processes. Next, we use the uniform distribution as the PDF that describes the random positions  $x_s$ . In mathematical terms,

$$p_X(x_n) = \left( \frac{1}{L} \right) \text{rect} \left( \frac{x_n}{L} \right). \quad (22)$$

In Eq. (22) the upper-case letter  $L$  represents the width of the interval, where the random locations are contained. For the uniform distribution, the characteristic function is a real function

$$P_X(\beta) = \int_{-\infty}^{\infty} p_X(x_n) \exp(-i 2\pi \beta x_s) dx_s. \quad (23)$$

$$P_X(\beta) = \text{sinc}(L\beta)$$

Then, in this case, the visibility of the Lau fringes is a real function,

$$\gamma(L) = \text{sinc} \left( \frac{4Ld}{\lambda f} \right). \quad (24)$$

In Fig. 7(a), we display the random positions (in arbitrary units) of 1000 mutually incoherent point sources, inside the source plane  $X_s$ - $Y_s$ . For emphasizing the statistical behavior of these locations, in Fig. 7(b) we show the histogram of the different values of the horizontal coordinate,  $X_s$ . These horizontal positions can be described as a random process, which obeys a uniform probability density function.

In Fig. 8, we plot the visibility function in Eq. (24) as a red color curve. And as a series of blue points, we depict the average visibility; that is, the value of the visibility obtained by evaluating the average irradiance distribution in Eq. (21). For our numerical simulations, we assume that the grating has period equal to 1 mm, the lens has a focal length  $f = 200$  mm, and the wave length is  $\lambda = 632.991$  nm. Along

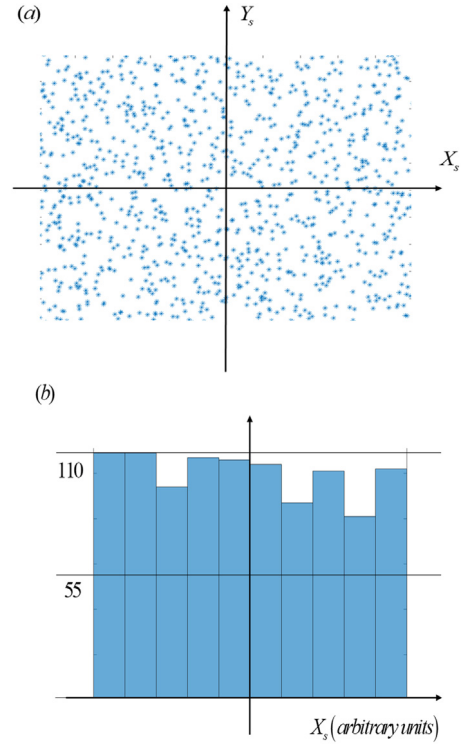


Fig. 7. Numerical simulations of the locations of a cluster of 1000 mutually incoherent point sources. In (a) we depict the positions (in arbitrary units) inside the source plane; in (b) we show the histogram of the values taken by the horizontal coordinate  $X_s$ .

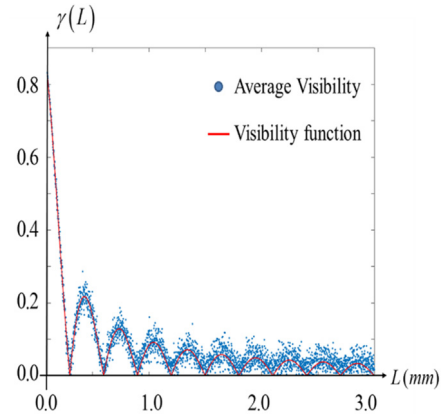


Fig. 8. Graph of the visibility function, red curve, and the numerical simulation of average visibility, as blue points, of the overall superimposed irradiance patterns.

the horizontal axis, we vary the values of  $L$  in units of millimeters. From Eq. (24) and from Fig. 8, we note that the values of the visibility function are greater than one tenth of its maximum value provided that

$$L \leq \left( \frac{10}{11} \lambda \right) \left( \frac{f}{d} \right). \quad (25)$$

Next, we employ a Gaussian distribution as the probability density function of the random process. This distribution is centered at the origin of the  $x$ -axis, then

$$p_X(x_s) = \frac{1}{L\sqrt{2\pi}} \exp \left[ -\frac{1}{2} \left( \frac{x_s}{L} \right)^2 \right]. \quad (26)$$

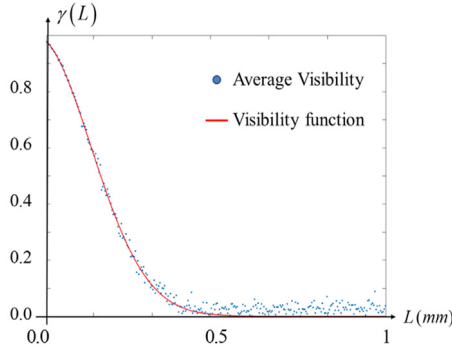


Fig. 9. Same as Fig. 8, but for a Gaussian distribution as the probability density function of the random process.

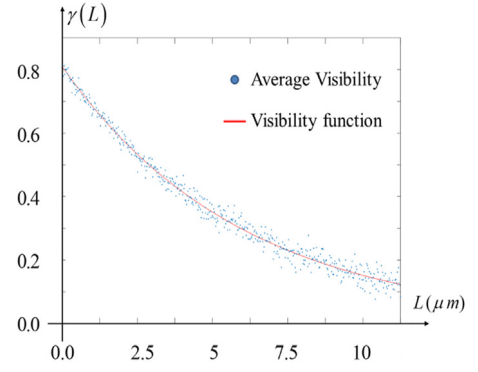


Fig. 10. Same as Fig. 8, but for a Lorentzian distribution.

Now, in Eq. (26) the upper-case letter L denotes the standard deviation. For this case, the characteristic function is again a real function

$$P_X(\beta) = \exp(-2(\pi L \beta)^2). \quad (27)$$

Then, the visibility function of the Lau fringes is

$$\gamma(L) = \exp\left[-2\left(\frac{2\pi d}{\lambda f}\right)^2 L^2\right] \quad (28)$$

In Eq. (28) the upper-case letter L has dimensions of length, and its variations are measured in millimeters (see Figs. 6, 9 and 10).

Here we note that the values of the visibility function are greater than one tenth of its maximum value, provided that

$$L \leq \left(\frac{\lambda}{5}\right) \left(\frac{f}{d}\right). \quad (29)$$

Again, the result in Eq. (29) may be seen as a tolerance criterion on the spread of the point sources, along the  $x$ -axis. For a grating with period equal to 1 mm, a lens with focal length  $f = 200$  mm, and for  $\lambda = 600$  nm, we have that  $L \leq 24 \mu\text{m}$ . From the above results we can infer that one can tailor the visibility variations by selecting a source suitable composed by a set of mutually incoherent point sources, which obey a specific PDF. For example, let us consider that one wishes to obtain visibility variations falling as a linear exponential curve,

$$\gamma(L) = \exp\left[-8\pi \frac{Ld}{\lambda f}\right]. \quad (30)$$

In Eq. (30) the upper-case letter L has dimensions of length, and its variations are measured in microns. Then, in Eq. (30) the damping coefficient is equal to  $8\pi d/(\lambda f)$ ; which has dimensions of 1/length. The set of mutually incoherent point sources should have random locations, following a Lorentzian PDF; that is

$$p_X(x_s) = \frac{1}{\pi} \frac{L}{(x_s^2 + L^2)}. \quad (31)$$

For a grating with period equal to 1 mm, a lens with focal length  $f = 200$  mm, and for  $\lambda = 600$  nm, we have that  $L \leq 24 \mu\text{m}$ .

In the next section, we analyze the impact of time average on the visibility of the Lau fringes.

#### 4. Time average OTF

As is depicted in Fig. 11, we consider now that inside the source plane, a point source moves following a harmonic motion with time period  $T$  and amplitude  $L$ . Then, any time the  $x$  coordinate of the point source is

$$x_s(t) = L \sin\left(2\pi \frac{t}{T}\right). \quad (32)$$

Trivially, In Eq. (32) the amplitude of the harmonic motion is equal to  $L$ , which has dimensions of length; and angular velocity is  $\omega = 2\pi/T$ .

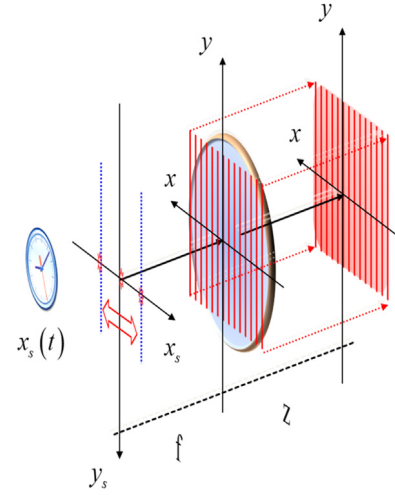


Fig. 11. Schematics of the optical setup that describes a point source moving harmonically along the horizontal axis of the source plane.

For the sake of simplicity of our discussion, in what follows we assume that the point source does not have any motion along the vertical axis.

From Eqs. (6) and (32) we have that the generation of the Lau fringes can be described by defining the instantaneous OTF

$$H(\mu, \nu; t) = \frac{1}{2} \delta(\mu) \delta(\nu) + \frac{1}{4} \delta\left(\mu + \frac{2}{d}\right) \delta(\nu) \exp\left[-i2\pi L \beta \sin\left(2\pi \frac{t}{T}\right)\right] + \frac{1}{4} \delta\left(\mu - \frac{2}{d}\right) \delta(\nu) \exp\left[i2\pi L \beta \sin\left(2\pi \frac{t}{T}\right)\right] \quad (33)$$

Now, if one applies the Bessel–Jacobi expansion, and by considering that the Lau fringes are recorded with a detector (which takes a time  $\tau$  for gathering the image) then the average OTF is

$$\langle H(\mu, \nu) \rangle = \frac{1}{2} \delta(\mu) \delta(\nu) \frac{1}{\tau} \int_{t=-\frac{\tau}{2}}^{\frac{\tau}{2}} dt + \frac{1}{4} \delta\left(\mu + \frac{2}{d}\right) \delta(\nu) \sum_{m=-\infty}^{\infty} J_m(2\pi L \beta) \frac{1}{\tau} \int_{t=-\frac{\tau}{2}}^{\frac{\tau}{2}} \exp\left(-i2\pi \frac{m}{T} t\right) dt + \frac{1}{4} \delta\left(\mu - \frac{2}{d}\right) \delta(\nu) \sum_{m=-\infty}^{\infty} J_m(2\pi L \beta) \frac{1}{\tau} \int_{t=-\frac{\tau}{2}}^{\frac{\tau}{2}} \exp\left(i2\pi \frac{m}{T} t\right) dt. \quad (34)$$

Next, it is straightforward to show that Eq. (34) becomes

$$\langle H(\mu, \nu) \rangle = \frac{1}{2} \delta(\mu) \delta(\nu) + \frac{1}{4} \left\{ \sum_{m=-\infty}^{\infty} J_m(2\pi L \beta) \text{sinc}\left[\frac{\tau}{T} m\right] \right\} \left[ \delta\left(\mu + \frac{2}{d}\right) + \delta\left(\mu - \frac{2}{d}\right) \right] \delta(\nu). \quad (35)$$

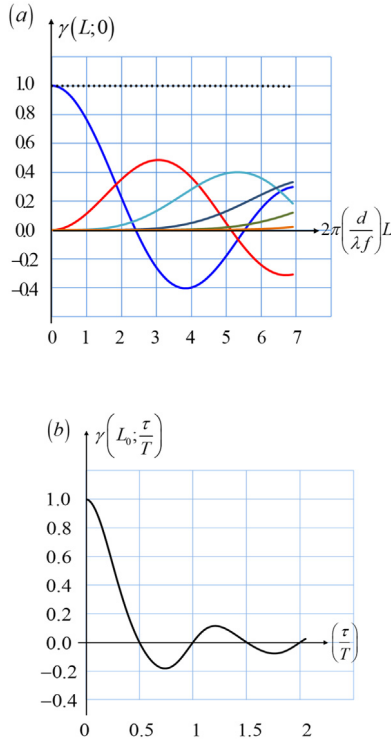


Fig. 12. Visibility functions as described in Eqs. (37) and (40).

By taking the inverse Fourier transform of Eq. (35), we obtain that average irradiance distribution of the Lau fringes is

$$\langle I(x, y) \rangle = \frac{1}{2} + \frac{1}{2} \left\{ \sum_{m=-\infty}^{\infty} J_m \left( 2\pi \frac{Ld}{\lambda f} \right) \text{sinc} \left[ \frac{\tau}{T} m \right] \right\} \cos \left( 4\pi \frac{x}{d} \right). \quad (36)$$

Thus, the visibility of the Lau fringes reads

$$\gamma \left( L; \frac{\tau}{T} \right) = J_0 \left( 2\pi \frac{Ld}{\lambda f} \right) + 2 \sum_{m=1}^{\infty} J_{2m} \left( 2\pi \frac{Ld}{\lambda f} \right) \text{sinc} \left[ 2 \frac{\tau}{T} m \right]. \quad (37)$$

It is apparent from Eq. (37) that the first term is not related to the time mismatching between the averaging time  $\tau$ , and the time period  $T$ . We also note that for  $\tau = 0$  the visibility function is equal to unity. Moreover, from Eq. (37), we recognize that if the ratio  $2\tau/T$  is an integer number, say  $n$ , then

$$\gamma(L; n) = J_0 \left( 2\pi \left( \frac{d}{\lambda f} \right) L \right). \quad (38)$$

As is depicted in Fig. 12(a). It is convenient then to set a condition for eliminating the first term in Eq. (37). To this end, we set

$$2\pi \frac{d}{\lambda f} L_0 = 2.4048. \quad (39)$$

Under this condition, the visibility of the Lau fringes depends only on the mismatching between the averaging time  $\tau$  and the time period  $T$ . In mathematical terms,

$$\gamma \left( L_0; \frac{\tau}{T} \right) = 2 \sum_{m=1}^{\infty} J_{2m} (2.4048) \text{sinc} \left[ 2m \frac{\tau}{T} \right]. \quad (40)$$

For visualizing the above results, in Fig. 12(a) we plot the initial terms of the visibility function, as well as the sum of those terms, when setting  $\tau = 0$  in Eq. (37). And in Fig. 12(b) we plot Equation (40).

From the previous results, we recognize that the visibility of the Lau fringes can be exploited as a null test for sensing any mismatching between the averaging time  $\tau$  and the time period  $T$ , in a somehow similar technique to stroboscopic illumination [17].

## 5. Final remarks

For three different source architectures, we have analyzed the visibility changes of the irradiance periodic patterns, which are obtained in the Lau effect. If you will, in the noncoherent Talbot effect.

We have related the visibility variations, of the Lau fringes, with the path that follows a very narrow slit, under incoherent illumination. We have defined a visibility complex function that varies with the geometrical bends of a slit source.

We have indicated that one can exploit the above result for setting a test that verifies the straightness of a slit source, under noncoherent illumination. We have reported some numerical simulations.

Next, we have related the visibility of the Lau fringes with the random locations of a set of mutually incoherent point sources. We have shown that the characteristic function, of the random process, specifies the visibility function of the Lau patterns.

We have also discussed the visibility variations, in the Lau patterns, which are caused by taking long exposure pictures of point source that moves periodically along the horizontal axis of the source plane. We have defined a time average OTF for finding an analytical expression that relates the visibility with the mismatch between the integration time  $\tau$  and the period of the harmonic motion.

In a somehow similar technique to stroboscopic illumination, we have suggested a null test for sensing any mismatches between the averaging time  $\tau$  and the time period  $T$ .

## Acknowledgment

We are indebted to the reviewer for her/his sound comments; which were very helpful for improving our manuscript.

## References

- [1] A.A. Michelson, *Studies in Optics*, The University of Chicago Press, Chicago, 1927, p. 31.
- [2] F. Zernike, *Physica* 5 (1938) 785–795.
- [3] H.H. Hopkins, *Proc. R. Soc. Ser. A* 208 (1951) 263–277.
- [4] G.L. Rogers, *Noncoherent Optical Processing*, John Wiley, 1977, p. 106.
- [5] E. Lau, *Ann. Phys.* 6 (1948) 417.
- [6] Jürgen Jahns, Adolf W. Lohmann, *Opt. Commun.* 28 (3) (1979) 263.
- [7] R. Sudol, Brian J. Thompson, *Opt. Commun.* 31 (2) (1979) 106.
- [8] F. Gori, *Opt. Commun.* 31 (1979) 4.
- [9] K.-H. Brenner, A.W. Lohmann, J. Ojeda-Castañeda, *Opt. Commun.* 46 (1) (1983) 14.
- [10] G.J. Swanson, E.N. Leith, *J. Opt. Soc. Amer.* A 4 (1985) 789.
- [11] Jorge Ojeda-Castañeda, Jorge Ibarra, Juan Carlos Barreiro, *Opt. Commun.* 71 (3, 4) (1989) 151–155.
- [12] Jorge Ojeda-Castañeda, E. Enrique Sicre, *Opt. Commun.* 59 (2) (1986) 87.
- [13] Pedro Andrés, Jorge Ojeda-Castañeda, Jorge Ibarra, *Opt. Commun.* 60 (4) (1986) 206.
- [14] Jorge Ojeda-Castañeda, Pedro Andrés, Jorge Ibarra, *Opt. Commun.* 67 (4) (1988) 256.
- [15] S. Chitralekha, K.V. Avudainayagam, S.V. Pappu, *Appl. Opt.* 29 (1990) 125.
- [16] B.R. Frieden, *Probability, Statistical Optics, and Data Testing*, Springer-Verlag, 1991, pp. 218–224.
- [17] J.S. Harris, R.L. Fusek, J.S. Marcheski, *Appl. Opt.* 18 (1979) 2368–2371.